The *H19* locus acts *in vivo* as a tumor suppressor

Tomomi Yoshimizu*†, Audrey Miroglio*†, Marie-Anne Ripoche*, Anne Gabory*, Maria Vernucci‡, Andrea Riccio‡, Sabine Colnot§, Cécile Godard§, Benoit Terris§, Hélène Jammes*, and Luisa Dandolo*¶

*Department of Genetics and Development and §Department of Endocrinology, Metabolism and Cancer, Institut Cochin, University Paris Descartes, Centre National de la Recherche Scientifique Unité Mixte de Recherche 8104, Institut National de la Santé et de la Recherche Médicale U567, Paris 75014, France; and ‡Department of Environmental Science, Second University of Naples and Institute of Genetics and Biophysics A. Buzzati Traverso, CNR, Naples 81100, Italy

Edited by Benjamin Tycko, Department of Pathology, Institute of Cancer Genetics, New York, NY, and accepted by the Editorial Board June 18, 2008 (received for review February 15, 2008)

The *H19* locus belongs to a cluster of imprinted genes that is linked to the human Beckwith-Wiedemann syndrome. The expression of *H19* and its closely associated *IGF2* gene is frequently deregulated in some human tumors, such as Wilms' tumors. In these cases, biallelic *IGF2* expression and lack of expression of *H19* are associated with hypermethylation of the imprinting center of this locus. These observations and others have suggested a potential tumor suppressor effect of the *H19* locus. Some studies have also suggested that *H19* is an oncogene, based on tissue culture systems. We show, using *in vivo* murine models of tumorigenesis, that the *H19* locus controls the size of experimental teratocarcinomas, the number of polyps in the *Apc* murine model of colorectal cancer and the timing of appearance of SV40-induced hepatocarcinomas. The *H19* locus thus clearly displays a tumor suppressor effect in mice.

genomic imprinting | *Igf2* | murine models

The *H19-Igf2* locus is subject to genomic imprinting and has often been used as a paradigm for the study of this particular epigenetic regulation. The *H19* locus produces a 2.5-kb noncoding, spliced, and polyadenylated RNA of yet-unknown function (1, 2). The *Igf2* gene encodes a fetal growth factor, insulin-like growth factor 2. These two genes are located 90 kb apart and are oppositely imprinted: *H19* is maternally expressed and *Igf2* paternally expressed (1, 3). They belong to a large imprinted domain localized on chromosome 7 in mice and chromosome 11p15.5 in humans. The imprinting of *Igf2* and *H19* is controlled by a region located 4 kb upstream from the *H19* transcription unit, defined as the *H19* differentially methylated region (DMR) or imprinting control region (ICR) (4).

The 11p15.5-imprinted domain is linked to the Beckwith-Wiedemann syndrome (BWS), which is characterized by overgrowth phenotypes of affected children as well as a predisposition to develop embryonal tumors such as Wilms' tumor or rhabdomyosarcomas (5). Among the molecular alterations involved in BWS, certain cases (20%) show paternal uniparental disomy (UPD); other cases (5–10%) have hypermethylation of the *H19* DMR; and both lead to lack of expression of *H19* as well as activation of *IGF2*. These patients have higher risk of developing tumors than patients with other molecular defects (6). Genetic and epigenetic alterations at 11p15.5 similar to those found in the BWS have also been demonstrated in nonsyndromic Wilms' tumors. A great number of these cases have either loss of the maternal allele (LOH) or LOI (7, 8). It has thus been suggested that the *H19* gene could have a possible tumor suppressor function (9). The first direct evidence for this tumor suppressor function was provided by *in vitro* experiments in which transfection of *H19* cDNA into G401-transformed kidney cells resulted in loss of tumorigenicity of these cells (10). Subsequent experiments performed with *in vitro* culture systems suggested that *H19* played a role as an oncogene rather than a tumor suppressor gene (11, 12). This controversy has not yet been resolved, as numerous human tumors have been shown to display either overexpression or lack of *H19* expression (13–15).

We decided to investigate the potential role of the *H19* locus *in vivo* by producing murine models of tumorigenesis. We used *H19*Δ*3* (16) and *H19*Δ*Enh* (17) mice (Fig. 1*A*) and 3 distinct models of tumorigenesis to investigate the potential tumor suppressor activity of the *H19* locus. In the first model, experimental teratocarcinomas induced by grafting embryos under the kidney capsule were compared for size, weight, and histopathology (18). In the second model, the *H19*Δ*3* mice were bred with mutants of the *Apc* gene, *Apc*Δ*14*/+, which represent a murine model for colorectal cancer (19). The double mutants lacking *H19* and *Apc* show an increase in number of polyps compared with their *Apc* littermates. Finally, using a transgenic SV40 hepatocarcinoma model (20, 21), we show that the delay of appearance of these tumors is greatly reduced in the absence of *H19*. Interestingly, these models derive from the 3 germ layers (endoderm, mesoderm, and ectoderm) and result in similar phenotypes, showing a tumor suppressor function for the *H19* locus.

Results

Teratocarcinoma Model. ***H19*Δ*3* phenotype and *Igf2* expression.** We originally described that in the *H19*Δ*3* mutants the maternal *Igf2* allele was slightly reexpressed in skeletal muscle but not in liver (16). To identify the precise levels of *Igf2* expression, we extended our analysis to other organs using a cross between *H19*Δ*3* and *SD7* mice. *Igf2* is biallelically expressed only in mesoderm-derived tissues (limb muscle, tongue, diaphragm, and heart) and not in endoderm-derived tissues (kidney, lung, and liver) (Fig. 1*B*). Importantly, maternal *Igf2* reexpression reaches at most 20–30% of the paternal allele in 5-day neonates, showing that there is only a slight increase in *Igf2* mRNA levels in the *H19*Δ*3* mice.

Production of tumors on wt background. Experimental teratocarcinomas were produced by grafting E 6.5 embryos under the kidney capsule of syngenic mice. We first compared the weight of tumors obtained after grafting *wt* or *H19*Δ*3* embryos into *wt* recipient mice. The results showed a clear difference for the two genotypes (Fig. 2*A*). Although there was some heterogeneity, the overall weight of *H19*Δ*3* derived tumors was ≈1.6-fold higher than that of *wt*-derived tumors ($P = 0.015$).

In all cases, the tumor and the kidney were clearly individualized, with no invasion of the tumor into the kidney (Fig. 2*B*). Histologic analysis revealed the presence of different tissues derived from all 3 embryonic germ layers (ectoderm, endoderm, and mesoderm). There were no striking differences in the type of tissue, suggesting that the absence of *H19* does not affect the development of any 1 particular tissue and that all 3 germ layers are involved.

Author contributions: T.Y., A.M., M.-A.R., A.G., M.V., A.R., C.G., B.T., H.J., and L.D. performed research; T.Y., A.M., M.-A.R., A.G., M.V., A.R., B.T., H.J., and L.D. analyzed data; A.R. and L.D. designed research; S.C. and C.G. contributed new reagents/analytic tools; and A.R. and L.D. wrote the paper.

The authors declare no conflict of interest.

This article is a PNAS Direct Submission. B.T. is a guest editor invited by the Editorial Board.

†T.Y. and A.M. contributed equally to this work.

¶To whom correspondence should be addressed at: Department of Genetics and Development, Institut Cochin, 24 rue Fbg St Jacques, Paris 75014, France. E-mail: luisa.dandolo@cochin.inserm.fr.

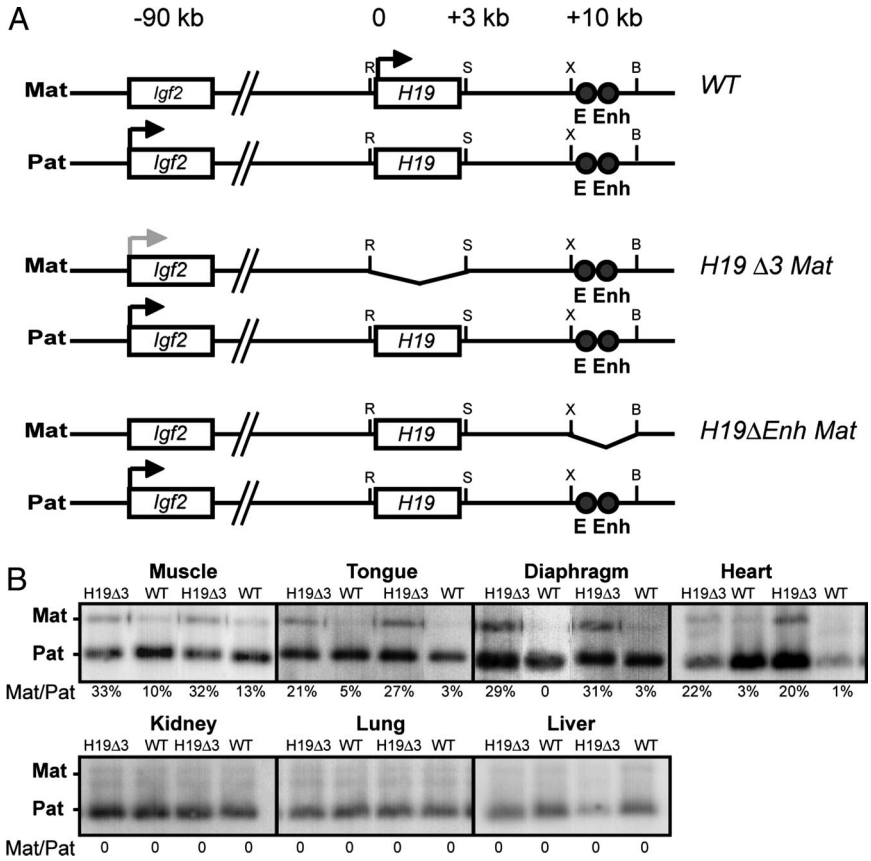

Fig. 1. Expression of the *H19-Igf2* locus. (*A*) Maps of the *H19-Igf2* locus. *Wt*, *H19Δ3* and *H19Δenh* mutants are represented with maternal (Mat) and paternal (Pat) alleles. Endodermal enhancers (E Enh) are indicated downstream from the *H19* gene. Black arrows indicate full transcription and the gray arrow indicates weak transcription. R = EcoRI, S = SalI, X = XbaI, B = BamHI. (*B*) *Igf2* expression analysis in *H19Δ3* and *wt* mesoderm- and endoderm-derived organs. *H19Δ3* and *wt* females were crossed with *SD7* males. Semiquantitative RT-PCR was performed on 2 organ samples of 5-day-old mice, then digested with *BsaA1* to detect the *Mus spretus* paternal polymorphism. Maternal *Igf2* expression was only detected in mesoderm derived tissues, as shown by the Mat/Pat ratio under each slot.

Production of tumors on Igf2$^{-/-}$ background. To separate paracrine and autocrine effects of IGF2, we performed the same grafting experiment using *Igf2*$^{-/-}$ recipient mice. There was a strong reduction in the overall size of the tumors for both genotypes (Fig. 2*A*), suggesting that circulating IGF2 in the recipient mouse plays an important role in the final size of the tumors. Most interestingly, the relative weight difference was maintained, with a 2-fold difference between *H19Δ3* tumors compared with *wt* tumors on this *Igf2*$^{-/-}$ background ($P < 0.05$).

Taken together, analysis of the weight of the tumors at 35 days on both *wt* and *Igf2*$^{-/-}$ backgrounds showed a significant difference according to their genotype, with the *wt* tumors being smaller than the *H19Δ3*-derived tumors. Because the relative weight difference between the two genotypes (*wt* and *H19Δ3*) was maintained on both backgrounds (*wt* and *Igf2*$^{-/-}$), this implies that the *H19* locus plays a definite role in the production of these experimental tumors.

Tumor Characteristics. ***H19 and Igf2 expression.*** We investigated the levels of *Igf2* mRNA by real-time quantitative RT-PCR in tumors produced both in the *wt* and the *Igf2*$^{-/-}$ host background. *Igf2* expression was heterogeneous, did not strictly correlate with tumor weight and showed no significant difference between *wt* and *H19*$^{-/-}$ derived tumors (Fig. 2*C*). We concluded from these results (*i*) that tumor size is controlled by presence or absence of the *H19* locus with little correlation to autocrine levels of *Igf2* expression, and (*ii*) that the host background and the level of paracrine IGF2 play a major role in tumor size. Whether this effect is due to the protein itself or to other factors under the control of the *Igf2* gene remains to be elucidated.

Methylation status of H19 ICR. Because hypermethylation of the *H19* DMR has been observed in Wilms' tumor samples, we investigated its methylation state in our teratocarcinoma samples. Tumor DNA was digested with SacI and HhaI (a methylation-sensitive enzyme) and the methylation state of the ICR was analyzed using a probe overlapping 1 of the CTCF binding sites (CTCF site 3) (Fig. 2*D*). These results were quantified and show a slightly higher methylation index (MI; methylated fragment/methylated plus unmethylated fragment) than expected but no significant difference between the two types of tumors. There was therefore no striking shift in the pattern of methylation of the *H19* ICR.

The results obtained from this teratocarcinoma study suggest that the lack of *H19* expression leads to larger tumors, consistent with its proposed role of tumor suppressor, and independently of *Igf2* levels of expression.

Colorectal Cancer Model. ***Increased adenoma number in the H19Δ3/+Apc^{Δ14}/+ mutant mice.*** To study the effect of absence or presence of the *H19* locus in a murine carcinogenesis model, we bred *H19Δ3* heterozygous females (outbred C57BL/6/CBA) with the *Apc^{Δ14}* heterozygous males. This cross produced 4 genotypes, *H19+/+Apc+/+* (*wt*), *H19Δ3/+Apc+/+*, *H19+/+Apc^{Δ14}/+* and *H19Δ3/+Apc^{Δ14}/+*. Because of genomic imprinting, *H19Δ3/+* progeny completely lack *H19* expression. Mice were analyzed at 180 days, as some began to show signs of anemia and rectal bleeding with prolapse. As expected, in the absence of *Apc* mutation, no polyps were detected in the *wt* and *H19Δ3/+Apc+/+* mice. In *Apc^{Δ14}/+* mice, the number of adenomas was significantly higher (2.2-fold)

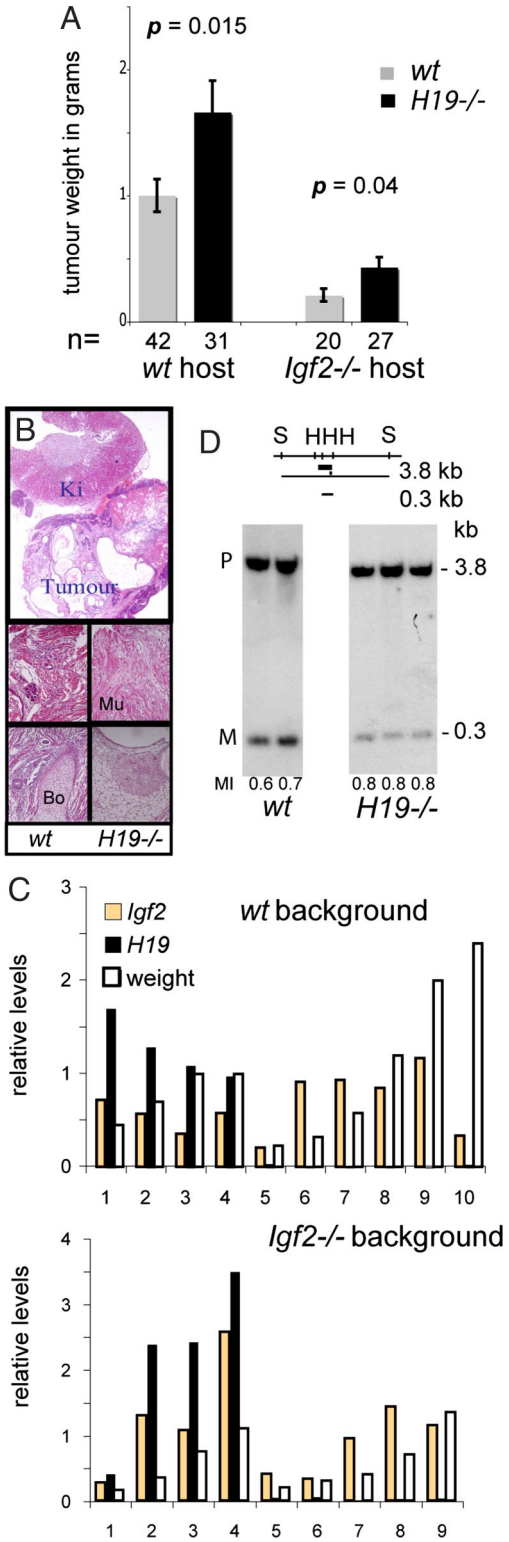

Fig. 2. Teratocarcinoma model. (*A*) Diagram of weights from *wt* and H*19Δ3* derived tumors 35 days after grafting. *Wt* and H*19Δ3* (indicated as $H19^{-/-}$) are plotted in gray and black respectively, either on *wt* or $Igf2^{-/-}$ recipient background. (*B*) Histologic sections of embryo-derived teratocarcinomas. Tumor section after ectopic grafting to the kidney (*Top*). Differentiated tissues such as muscle (*Middle*) or bone (*Bottom*) in both *wt* and *H19Δ3* derived tumors can be identified. (*C*) Expression analysis of *Igf2* in tumors. Levels of *Igf2* mRNA (orange) were determined by real-time qRT-PCR in *wt* and $H19^{-/-}$ derived tumors, produced on *wt* or $Igf2^{-/-}$ recipient background. *H19* levels are shown in black (samples 1–4 are *wt*, others are $H19^{-/-}$). In each set of samples, tumors are displayed by increasing weight as indicated in white. No significant difference in the levels of *Igf2* was detected between the 2 sample sets ($P = 0.39$ on *wt* hosts and $P = 0.45$ on $Igf2^{-/-}$ hosts, respectively). (*D*) Methylation status of the ICR in tumors. Tumor DNA (*wt* in *Left* and *H19Δ3* in *Right*) was digested with SacI (*S*) and HhaI (*H*) and analyzed with the CTCF3 probe (thick black line). The resulting 3.8 kb SacI fragment corresponds to the fully methylated paternal allele and the 0.3 kb HhaI fragment to the unmethylated maternal allele. Methylation index (MI) is indicated under each sample.

in the absence of *H19* than in its presence ($P = 0.05$) (Fig. 3*A*). Strikingly, the increase in the number of smaller polyps (<2 mm) was even greater (3-fold difference) in the absence of *H19*. This would suggest that the *H19* locus could control the initiation step of tumorigenesis.

We performed the same cross using females carrying the *H19Δ3* mutation on the 129/SvPas background. A similar increase in number of adenomas (1.4-fold) in mice lacking the *H19* locus was detected. This difference (1.4- vs. 2.2-fold) is consistent with observations suggesting the presence of modifier genes in the 129 strain compared with the C57BL/6 background (22).

Histology of the intestinal lesions. Close histologic examination of the whole-intestine "Swiss rolls" revealed the presence of adenomas, with some *in situ* adenocarcinomas (Fig. 3*B*), which occurred independently from the presence or absence of the *H19* locus.

Previous experiments describing the effect of another *H19* mutation, *H19Δ13* (in which *Igf2* mRNA level is increased by 2-fold) on tumor incidence in the *Apc min* mice had shown that an increase in crypt length was observed due to the increased level of IGF2 (23, 24). To exclude a role for IGF2 in the polyps produced in the *H19Δ3* mutants, we evaluated the crypt size on hematoxylin and eosin(H&E) -stained sections of the small intestine, by performing 16 measures per section of *H19+/+Apc*Δ*14/+* ($n = 5, 3$ on C57BL/6 and 2 on 129/SvPas background) and *H19Δ3/+Apc*Δ*14/+* mice ($n = 5$, 2 on C57BL/6 and 3 on 129/SvPas background) (Fig. 3*B*). No difference in crypt length was found, with an average of 2.8 units for the *H19+/+Apc*Δ*14/+* mice and of 2.6 units for the *H19Δ3/+Apc*Δ*14/+* mice (a control *wt* mouse had a 2.8-unit crypt length). These data suggest that the levels of *Igf2* expression did not differ between the *wt* and the *H19Δ3* genotypes and did not affect intestinal growth in these mice.

Igf2 expression levels. To confirm the absence of effect of the *Igf2* gene, we compared the levels of *Igf2* expression between *wt* and *H19Δ3* strains by semiquantitative and real-time qRT-PCR. *Igf2* expression is very low in colon and intestine in *H19Δ3/+* as well as in *wt* mice, compared with muscle, where it is highly expressed (data not shown). *Igf2* expression is also very low and heterogeneous in polyps from both *H19Δ3/+Apc*Δ*14/+* and *H19+/+Apc*Δ*14/+* mice, with no significant difference between the two genotypes ($P = 0.06$) (Fig. 3*C*).

ICR methylation analysis. We also investigated whether the methylation status of the *H19* ICR was disrupted in the intestine, colon, and polyp DNA from these mice. The *H19* ICR displayed a constant methylation pattern, with the methylation index showing no significant difference between all genotypes and tissues analyzed (Fig. 3*D*).

Taken together, these results show that the lack of *H19* expression causes an increase in the number of polyps in the *Apc* colorectal cancer model, independent of *Igf2* expression. Interestingly, the initiation step of polyp appearance seems to be affected by the absence of *H19*.

Experimental Liver Carcinogenesis. ***Tumor formation.*** In mice carrying a targeted deletion of the endodermal enhancers located downstream from the *H19* gene (*H19ΔEnh*) (17), it was shown that these enhancers are required in *cis* for the activation of *Igf2* and *H19* during liver carcinogenesis (20). To establish whether *H19* had a

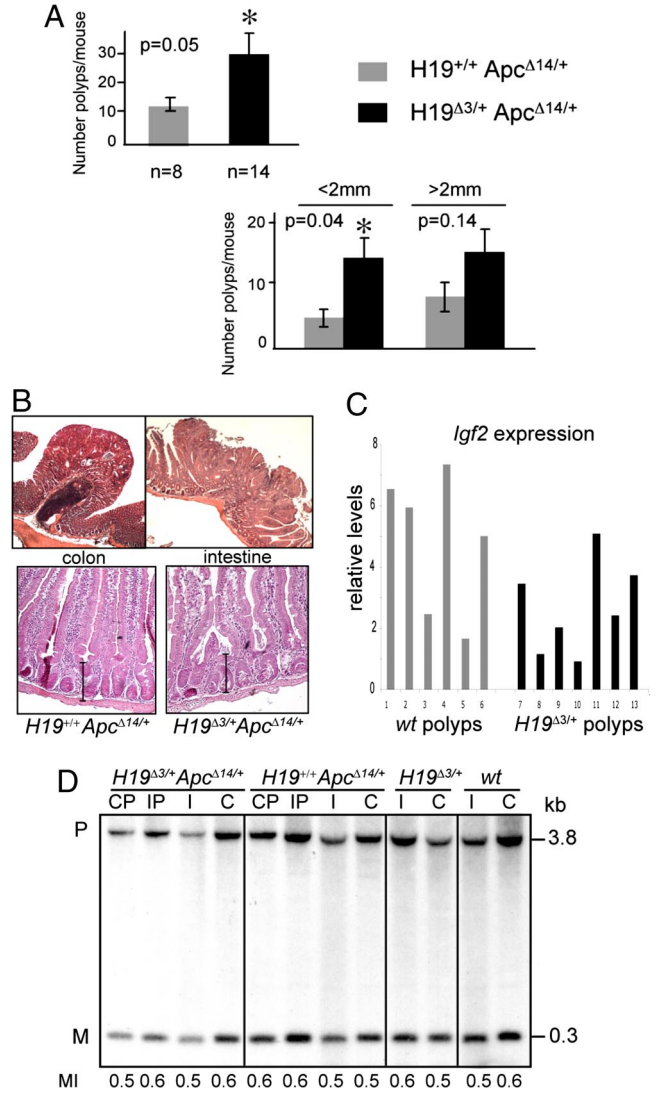

Fig. 3. Colorectal cancer model. (*A*) Effect of *H19* deletion on *Apc∆14/+* intestinal polyps at 180 days. *Top* shows the number of polyps in *H19+/+Apc∆14/+* (gray) and *H19∆3/+Apc∆14/+* (black) mice on C57BL/6 background ($P = 0.05$). *Bottom* shows the number of polyps smaller and larger than 2 mm for both genotypes, with a significantly higher number of smaller polyps in the *H19∆3/+Apc∆14/+*mice. (*B*) Histologic analysis. *Top* shows H&E staining of adenomas in the colon and small intestine of *H19∆3/+Apc∆14/+* mouse. *Bottom* shows H&E staining of the small intestine crypts from *H19+/+Apc∆14/+* and *H19∆3/+Apc∆14/+* mice. Crypt length was measured (black vertical bar) and showed no significant difference between the two genotypes. (*C*) Expression analysis of *Igf2* transcripts. Detection of *Igf2* transcript level by quantitative RT-PCR in polyps from *H19+/+Apc∆14/+* and *H19∆3/+Apc∆14/+* mice. *Gapdh* was used as control. (*D*) Methylation status of the ICR in intestine (I), colon (C), colon polyps (CP) and intestine polyps (IP) from *H19∆3/+Apc∆14/+*, *H19+/+Apc∆14/+*, *H19∆3/+* and *wt* mice. The 3.8-kb SacI fragment corresponds to the fully methylated paternal allele and the 0.3 kb HhaI fragment to the unmethylated maternal allele as in Fig. 2. Methylation indexes (MI) are indicated.

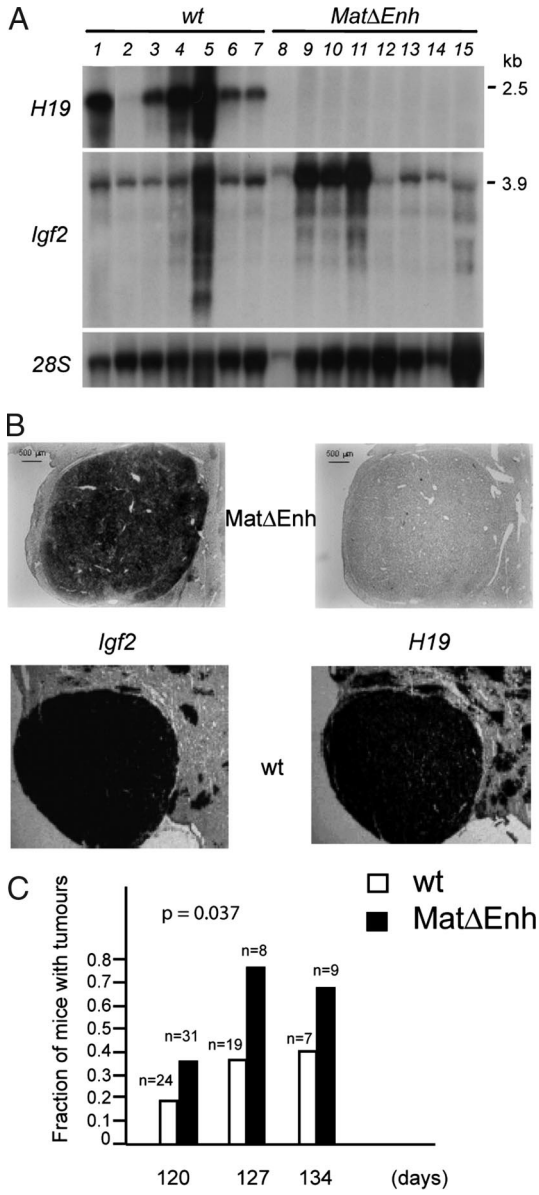

Fig. 4. Experimental liver carcinogenesis model. (*A*) Expression analysis of *Igf2* and *H19* transcripts. Northern analysis of 15 *wt* or *MatΔEnh* liver tumors. The blot was hybridized sequentially with the *H19*, *Igf2* and ribosomal *28S* probes. (*B*) *Igf2* and *H19* expression in *MatΔEnh* mice. Serial frozen sections of liver nodules of 148-day-old male *MatΔEnh* and *wt* mice were hybridized to S^{35}-labeled *Igf2* (*Left*) or *H19* (*Right*) probes. (*C*) Latency of liver tumor appearance in the *MatΔEnh* mutants. Mice were killed between 120 and 134 days of age. The histogram shows the fraction of animals with liver tumors larger than 3 mm. The number of mice analyzed in each class is indicated above the columns.

role in tumor development, we analyzed liver carcinogenesis in mice lacking *H19* expression (*MatΔEnh*, Fig. 1*A*).

The model investigated was that in which mice of the *CRP-Tag 60-3* line carry the SV40 T antigen oncogene under the promoter of the liver-specific human C-reactive protein gene (25, 26). The males of this transgenic line have a low but constitutive expression of the SV40 T antigen, which, after formation of hyperplastic foci and neoplastic nodules, eventually leads to the development of multiple hepatocellular carcinomas at 4–5 months of age.

We have previously shown that *H19* is activated in the experimental hepatocellular carcinomas (20, 26). We have now analyzed the expression of *H19* and *Igf2* in the liver tumors arisen in *MatΔEnh* and *wt* mice. Northern and *in situ* hybridization analyses showed that *H19* RNA was undetectable in the *MatΔEnh* tumors but was activated in the majority of the neoplasms found in the *wt* mice (Fig. 4*A* and 4*B*). RNase protection analysis demonstrated that the majority of *wt* tumors had *H19* RNA levels at least 3 orders of magnitude higher than the *MatΔEnh* tumors (data not shown). As in the *wt* mice, *Igf2* was expressed at variable levels in all tumors with the *MatΔEnh* genotype (Fig. 4 *A* and *B*). RNase protection analysis on 15 *wt* and 15 *MatΔEnh* tumors demonstrated very similar *Igf2*

mRNA levels (4.72 ± 2.6 vs. 4.73 ± 1.6 arbitrary units, data not shown).

Latency of tumor development. The male mice which developed liver tumors larger than 3 mm by 120 days of age were 11/31 (35%) for the *Mat*Δ*Enh* and 5/24 (20%) for the *wt* genotypes, respectively. By 127 and 134 days, the mice with tumors were 6/8 and 6/9 for the *Mat*Δ*Enh* genotype and 7/19 and 3/7 for the *wt* genotype, respectively (Fig. 4*C*). Overall, 23/48 (48%) *Mat*Δ*Enh* and 15/50 (30%) *wt* male mice ($P = 0.037$) had liver tumors when analyzed between 120 and 134 days of age. In contrast, *Pat*Δ*Enh* mice, expressing high levels of *H19* but low levels of *Igf2*, developed tumors with a delayed time course (20). These results suggest that the lack of *H19* expression causes acceleration in the development of liver tumors, consistent with its proposed role of tumor suppressor.

Discussion

The presence of a potential tumor suppressor gene in the 11p15.5 chromosomal region has been hypothesized for many years. This stemmed from the observation that in patients with BWS, there was a predisposition toward development of embryonal tumors. Two domains of imprinted genes have been identified in this region, the IC1 domain with the *H19-IGF2* locus and the IC2 domain with the *KCNQ1* locus associated with several other genes such as *CDKN1C* (or *p57KIP2*). The *H19* locus, with no known function was one of the candidates for a tumor suppressor (9).

The initial evidence in support of this hypothesis mainly involved *in vitro* experiments (10). Our aim was to use animal models to investigate the potential tumor suppressor activity of *H19 in vivo*. The *H19*Δ*3* mice we had produced never developed tumors, whatever background they were bred on (outbred C57BL/6/129 or inbred 129/SvPas). For this reason, we challenged these mutant mice in different tumor models.

The teratocarcinoma model has been an experimental system for producing tumors in the mouse which was described many years ago (27). Teratocarcinomas are composed of highly undifferentiated embryonal carcinoma (EC) cells and of differentiated cells derived from all 3 embryonic layers (mesoderm, endoderm, and ectoderm) (18). Teratocarcinomas can be produced either by grafting embryos or by injecting ES cells under the skin. We chose to graft E 6.5 embryos under the kidney capsule because this approach provided a better control of the number of grafted cells. We were aiming not only to investigate whether tumors were produced in presence or absence of *H19*, but also whether there was a size difference in these different cases.

The comparison of tumors induced by either *wt* or H*19*Δ*3* embryos clearly shows a difference in the weight of the tumors that are produced after 35 days. There is, of course, some heterogeneity, but overall H*19*Δ*3* tumors are larger than their *wt* counterparts. Importantly, the size difference between H*19*Δ*3* and *wt* induced teratocarcinomas was maintained on the $Igf2^{-/-}$ background (2-fold) compared with the *wt* background (1.6-fold).

These tumors displayed cells derived from endoderm, mesoderm, and ectoderm. This is interesting with regard to observations made on teratocarcinomas produced from androgenetic ES cells, which display lack of *H19* (maternally expressed) as well as disruption of many other imprinted genes (28). These tumors consisted predominantly of striated muscle. Since we find no difference in the type of tissues of *H19*Δ*3* or *wt* derived teratocarcinomas, the *H19* locus is probably not involved in the overproduction of muscle cells found in the androgenetic tumors. This could be of interest with respect to the occurrence of rhabdomyosarcomas in BWS patients and suggests that perhaps other genes of the 11p15.5 region are responsible for this type of tumor.

The choice of our second colorectal cancer model was prompted by data showing increase in size and number of polyps in mice carrying the *H19*Δ*13* mutation compared with *wt* mice (24). These mutant mice lack *H19* but also overexpress maternally derived *Igf2* because of the ICR deletion. To discriminate between the effects of each one of these genes, we performed the cross between *H19*Δ*3* females (in which the 3-kb transcription unit only is deleted) and *Apc* mutant males.

The number of polyps is >2-fold higher in absence of *H19*, with an increase in the number of small polyps, suggesting that lack of *H19* may play a role in the initiation step of tumorigenesis. Only low levels of *Igf2* mRNA were found in normal tissue (intestine and colon) and in the polyps, with no significant difference between mutant and *wt* polyps. No difference in the crypt size was detected, whereas previously published data suggested that relative levels of *Igf2* are responsible for crypt depth (24). Taken together, the results obtained from both our *H19*Δ*3* mutants and the *H19*Δ*13* mutants allow to postulate that *H19* is playing a definite role in the production and size of polyps, whereas *Igf2* may be contributing to the growth of these polyps by affecting the intestinal crypt size.

The SV40 induced hepatocarcinomas interestingly revealed an acceleration in the latency of appearance of the tumors in the absence of *H19* expression. Expression of the *Igf2* and *H19* genes is completely shut off in the liver of adult *CRP-Tag* mice, but is reactivated in a coordinate manner during liver carcinogenesis with conservation of their imprinted expression (26). In addition, loss of the maternal and duplication of the paternal copy of the chromosomal region bearing the *Igf2* and *H19* genes occur at high frequency in the hepatocellular carcinomas. These genetic events resemble the LOH occurring at chromosome 11p15.5 loci in human cancers and result in activation of *IGF2* and lack of *H19* expression.

It has been recently reported that the *H19* gene may act as an oncogene in studies using human cells maintained in culture and injected into mice to produce tumors (15). The discrepancy with our results could be explained by the difference in the systems. The main interest of our study resides in the use of mouse genetics. Our models reproduce a situation in which the potential oncogenic teratocarcinomas, $Apc^{-/+}$ polyps or SV40 induced hepatocarcinomas are challenged with mice in which the *H19* locus is present (or absent) throughout embryogenesis and the whole life of the mouse. Its effect is therefore constant and this may represent a more biologic situation than a cell culture system. It must also be acknowledged that the *H19* locus may play a more complex role in humans than in mice.

Because *H19* KO mice never spontaneously develop tumors *in vivo*, as other murine models of tumor suppressor genes, *H19* may play the role of a "modifier gene" suppressing tumorigenesis. It could act either through its long noncoding RNA or through the microRNA (miR-675) that has been recently described in exon 1 (29, 30). Targets of *H19* remain to be identified and linked to a biologic function possibly related to pathways involved in tumorigenesis.

Materials and Methods

Mouse Strains and Genotyping. The *H19*Δ*3* strain carries a 3kb deletion of the *H19* transcription unit and was initially established on an outbred C57BL/6/CBA background (16). Because an isogenic 129 background was required for the teratocarcinoma experiment, we also produced a 129 *H19*Δ*3* strain by reinjection of the original *H19*Δ*3*/+ ES cell line into blastocysts. The 129/SvPas *wt* strain and the 129 $Igf2^{-/-}$ strain (31) were used as recipients for the production of teratocarcinomas. The *H19*Δ*Enh* mice (17) were maintained on a C57BL/6 background. These mice can be bred as maternal heterozygotes (*MatH19*Δ*Enh*) which lack *H19* expression since the deletion is carried on the maternal allele (Fig. 1*A*). The *SD7* strain is a C57BL/6/CBA strain carrying the distal part of *Mus spretus* chromosome 7. The *Apc*Δ*14*/+ mice were bred on a C57BL/6 background (19) and were crossed with either the outbred *H19*Δ*3* or the inbred 129 *H19*Δ*3*. The *CRP-Tag 60-3* strain (25) was maintained on a BALB/c background. The protocol of animal handling and treatment was performed in accordance with the guidelines of the animal ethics committee of the Ministère de l'Agriculture of France.

Genotyping was done by PCR on tail DNA. Primers used for detecting the *H19*Δ*3* allele were *neo* primers: 5′ -GTCCTGATAGCGGTCCGCCA-3′ and 5′-GTGTTCCGGCTGTCAGCGCA-3′ (500 bp). The *Apc*Δ*14* allele was detected using primers that distinguish the *wt* allele (180 bp) from the exon14-excised allele (160

GENETICS

bp): Primer 1: 5′CTGTTCTGCAGTATGTTATCA-3′; Primer 2: 5′-CTATGAGTCAACA-CAGGATTA-3′; Primer 3: 5′-TATAAGGGCTAACAGTCAATA-3′.

Teratocarcinoma Production. Wt or *H19Δ3* embryos were dissected at 6.5dpc and the ectoplacental cone was taken off. These embryos were introduced under the kidney capsule of isogenic males (8–10 weeks old), as previously described (18). The recipient mice were either 129/SvPas *wt* or 129 *Igf2*$^{-/-}$ strain. 35 days after grafting, tumors were surgically dissected from the mice and weighed. A fraction of the tumor was used to prepare DNA and RNA. The remaining part was fixed in Bouin's fixative, embedded in paraffin, and 5 μm sections were stained with hematoxylin and eosin (H & E).

Polyp Analysis and Tumor Scoring. The progeny from the cross between *H19Δ3*/+ and *ApcΔ14*/+ mutant mice were killed at 180 days and genotyped. The entire intestinal tract was removed, flushed with PBS, and stained with Indigo carmine (0.08%). The small intestine and colon were opened longitudinally, flattened on filter paper, and fixed in 4% PFA. The number and size of the polyps were determined by double counting on mice blinded for genotype. The whole intestine was then rolled and embedded in paraffin for histologic analysis (''Swiss rolls''). Crypt length and tumor grading were performed on 5-μm H & E sections.

Analysis of Liver Tumorigenesis. Homozygous *CRP-Tag 60-3* males were mated with *MatH19ΔEnh* females, and liver carcinogenesis was analyzed in their progeny. The mice were genotyped for the presence of the *H19ΔEnh*, as described in ref. 21. The males were killed between 120 and 134 days of age. Livers were dissected from the mice and carefully examined for the presence of tumors. Only nodules larger than 3 mm were considered.

Statistical Analyses. Data are shown as averages and s.e.m. We used ANOVA analysis and Student *t* test with Excel X and Statview.

RNA Preparation and Analysis. Total RNA was extracted from 5-day neonate organs or tumors with TRIzol reagent (Invitrogen). For RT-PCR analysis, DNase I treated RNA (0.5 μg) was reverse-transcribed with SuperScript II and random hexamer primers (Invitrogen). For semiquantitative RT-PCR, 50 ng of cDNA were amplified using gene-specific primers and TaqDNA polymerase (Invitrogen) during 20 cycles. Detection of *Igf2* transcripts derived from the *SD7* cross was performed using primers: forward 5′-GACGTGTCTACCTCTCAGGCCGTACTT-3′ and reverse 5′ GGGTGTCAATTGGGTTGTTTAGAGCCA-3′. The 517-bp product was digested with *BsaA1*, yielding a 241-bp paternal fragment detected by the internal primer 5′- TCAAATTTGGTTTTTTAGAA-3′. RT-PCR products were separated on 1% agarose gels and transferred onto Hybond N+ membranes in 0.4 M NaOH. Blots were probed with γP^{32}ATP kinase-labeled primers at 42°C in Church buffer. Membranes were washed in 0.4×SSC, 0.5% SDS at 42°C and results were quantified using PhosphorImager analysis and ImageQuant software.

Quantitative q-PCR was performed on a Light Cycler system using Sybr Green PCR kits (Roche). 1 to 5 ng of cDNA were amplified in duplicate using primers for *H19*, *Igf2*, *GAPDH* and *TBP*. H19 F 5′-GGAGACTAGGCCAGGTCTC-3′; H19 R 5′-GCCCATGGTGTTCAAGAAGGC-3′; Igf2 F 5′-GGCCCCGGAGAGACTCTGTGC-3′; Igf2 R 5′-TGGGGGTGGGTAAGGAGAAAC-3′; GAPDH F 5′-ACAGTCCATGCCAT-CACTGCC-3′; GAPDH R 5′-GCCTGCTTCACCACCTTCTTG-3′; TBP F 5′-GCAATCAA-CATCTCAGCAACC-3′ and TBP R 5′-CGAAGTGCAATGGTCTTTAGG-3′. Genorm calculations were used for normalization.

Northern analysis and RNase protection assays were carried out as previously described (20).

Methylation Assay. DNA from tumors, polyps or control tissue was incubated at 55°C in lysis buffer (Tris 100 mM pH 8, EDTA 5 mM, SDS 0.2%, NaCl 20 mM, and 0.4 mg/ml Proteinase K (Sigma), followed by phenol-chloroform extraction and ethanol precipitation. DNA was digested with SacI and HhaI, separated on 1% agarose gels and transferred onto Hybond N + membranes. Southerns were probed with a 200-bp PCR product corresponding to the region covering the CTCF site No. 3: 5′ CTGTTATGTGCAACAAGGGAA and 3′ GGTCTTACCAGCCACTGA. Blots were washed at 65°C and quantified as described above.

***In situ* Hybridization.** *In situ* hybridization on liver sections was performed as previously described (26).

ACKNOWLEDGMENTS. We thank Arg Efstratiadis, Wolf Reik, and Shirley Tilghman for their kind gifts of *Igf2*$^{-/-}$ and *SD7* mice to L.D and *H19Δenh* mice to A.R. We thank Béatrice Romagnolo and Christine Perret for advice on the *ApcΔ14* colorectal cancer model. We are very grateful to Davor Solter, Jean Gaillard, and Michel Huerre for helpful comments and a critical eye on the teratocarcinoma sections. We thank Debra Wolgemuth and Edith Heard for constructive discussions on the manuscript. We thank Charles Babinet, Wolf Reik, and Azim Surani for constant encouragement. This work was supported by funding from the Ministère de la Recherche (ACI), Association de la Recherche contre le Cancer (ARC), Ligue contre le Cancer, Association Française contre les Myopathies (AFM), MIUR PRIN 2005 (AR), Istituto Superiore di Sanità (AR), Associazione Italiana Ricerca sul Cancro (AR), Telethon-Italia Grant GGP07086 (AR), and fellowships from ARC and AFM to A.M. and to T.Y.

1. Bartolomei MS, Zemel S, Tilghman SM (1991) Parental imprinting of the mouse H19 gene. *Nature* 351:153–155.
2. Gabory A, Ripoche MA, Yoshimizu T, Dandolo L (2006) The H19 gene: Regulation and function of a non-coding RNA. *Cytogenet Genome Res* 113:188–193.
3. DeChiara TM, Robertson EJ, Efstratiadis A (1991) Parental imprinting of the mouse insulin-like growth factor II gene. *Cell* 64:849–859.
4. Thorvaldsen JL, Duran KL, Bartolomei MS (1998) Deletion of the H19 differentially methylated domain results in loss of imprinted expression of H19 and Igf2. *Genes Dev* 12:3693–3702.
5. Weksberg R, Smith AC, Squire J, Sadowski P (2003) Beckwith-Wiedemann syndrome demonstrates a role for epigenetic control of normal development. *Hum Mol Genet* 12:R61–R68.
6. Cooper WN, *et al.* (2005) Molecular subtypes and phenotypic expression of Beckwith-Wiedemann syndrome. *Eur J Hum Genet* 13:1025–1032.
7. Moulton T, *et al.* (1994) Epigenetic lesions at the H19 locus in Wilms' tumor patients. *Nat Genet* 7:440–447.
8. Feinberg AP (1999) Imprinting of a genomic domain of 11p15 and loss of imprinting in cancer: An introduction. *Cancer Res* 59:1743s–1746s.
9. Rump P, Zeegers MP, van Essen AJ (2005) Tumor risk in Beckwith-Wiedemann syndrome: A review and meta-analysis. *Am J Med Genet A* 136:95–104.
10. Hao Y, Crenshaw T, Moulton T, Newcomb E, Tycko B (1993) Tumor-suppressor activity of H19 RNA. *Nature* 365:764–767.
11. Lustig-Yariv O, *et al.* (1997) The expression of the imprinted genes H19 and IGF-2 in choriocarcinoma cell lines. Is H19 a tumor suppressor gene? *Oncogene* 15:169–177.
12. Verkerk A, *et al.* (1997) Unique expression patterns of H19 in human testicular cancers of different etiology. *Oncogene* 14:95–107.
13. Dao D, *et al.* (1999) Multipoint analysis of human chromosome 11p15/mouse distal chromosome 7: Inclusion of H19/IGF2 in the minimal WT2 region, gene specificity of H19 silencing in Wilms' tumorigenesis and methylation hyper-dependence of H19 imprinting. *Hum Mol Genet* 8:1337–1352.
14. Frevel MA, Sowerby SJ, Petersen GB, Reeve AE (1999) Methylation sequencing analysis refines the region of H19 epimutation in Wilms tumor. *J Biol Chem* 274:29331–29340.
15. Matouk IJ, *et al.* (2007) The H19 non-coding RNA is essential for human tumor growth. *PLoS ONE* 2:e845.
16. Ripoche MA, Kress C, Poirier F, Dandolo L (1997) Deletion of the H19 transcription unit reveals the existence of a putative imprinting control element. *Genes Dev* 11:1596–1604.
17. Leighton PA, Saam JR, Ingram RS, Stewart CL, Tilghman SM (1995) An enhancer deletion affects both H19 and Igf2 expression. *Genes Dev* 9:2079–2089.
18. Damjanov I, Solter D, Skreb N (1971) Teratocarcinogenesis as related to the age of embryos grafted under the kidney capsule. *Wilhelm Roux' Archiv* 107:288–290.
19. Colnot S, *et al.* (2004) Colorectal cancers in a new murine model of familial adenomatous polyposis: Influence of genetic and environmental modifiers. *Lab Invest* 84:1619–1630.
20. Vernucci M, *et al.* (2000) The H19 endodermal enhancer is required for Igf2 activation and tumor formation in experimental liver carcinogenesis. *Oncogene* 19:6376–6385.
21. Vernucci M, *et al.* (2004) Developmentally regulated functions of the H19 differentially methylated domain. *Hum Mol Genet* 13:353–361.
22. Hassan AB, Howell JA (2000) Insulin-like growth factor II supply modifies growth of intestinal adenoma in Apc(Min/+) mice. *Cancer Res* 60:1070–1076.
23. Leighton PA, Ingram RS, Eggenschwiler J, Efstratiadis A, Tilghman SM (1995) Disruption of imprinting caused by deletion of the H19 gene region in mice. *Nature* 375:34–39.
24. Sakatani T, *et al.* (2005) Loss of imprinting of Igf2 alters intestinal maturation and tumorigenesis in mice. *Science* 307:1976–1978.
25. Ruther U, Woodroofe C, Fattori E, Ciliberto G (1993) Inducible formation of liver tumors in transgenic mice. *Oncogene* 8:87–93.
26. Casola S, *et al.* (1995) Loss of heterozygosity of imprinted genes in SV40 t/T antigen-induced hepatocellular carcinomas. *Oncogene* 11:711–721.
27. Stevens LC (1970) The development of transplantable teratocarcinomas from intratesticular grafts of pre- and postimplantation mouse embryos. *Dev Biol* 21:364–382.
28. Mann JR, Gadi I, Harbison ML, Abbondanzo SJ, Stewart CL (1990) Androgenetic mouse embryonic stem cells are pluripotent and cause skeletal defects in chimeras: Implications for genetic imprinting. *Cell* 62:251–260.
29. Mineno J, *et al.* (2006) The expression profile of microRNAs in mouse embryos. *Nucleic Acids Res* 34:1765–1771.
30. Cai X, Cullen BR (2007) The imprinted H19 noncoding RNA is a primary microRNA precursor. *RNA* 13:313–316.
31. DeChiara TM, Efstratiadis A, Robertson EJ (1990) A growth deficiency phenotype in heterozygous mice carrying an insulin-like growth factor II gene disrupted by gene targeting. *Nature* 345:78–80.